Study of a Circulation Control Airfoil with Leading/Trailing-Edge Blowing

B. G. McLachlan*
NASA Ames Research Center, Moffett Field, California

An experimental study of the flow past a two-dimensional circulation control airfoil under steady leading/trailing-edge blowing was conducted in a water tunnel. The effect of varying jet momentum on the flowfield was determined through the use of flow visualization and airfoil force measurements. The flow patterns associated with leading-edge blowing, alone and simultaneously with trailing-edge blowing, and with trailing-edge blowing alone, are described and correlated with the lift measurements. It was found that simultaneous blowing only results in a slight lift decrease in comparison to trailing-edge blowing alone. However, the number and complexity of the leading-edge flow patterns that can occur during simultaneous blowing are shown to be greater than previously thought. Furthermore, a pronounced unsteadiness in the lift generated is shown to occur for certain values of leading- and trailing-edge jet momentum.

Nomenclature

c = airfoil chord
C_ℓ = airfoil section lift coefficient, section lift/qc
C_μ = jet blowing momentum coefficient, $2(h/c)(U_j/U_\infty)^2$
h = jet slot height
q = freestream dynamic pressure, $(\frac{1}{2})\rho U_\infty^2$
Re = Reynolds number, based on airfoil chord, $U_\infty c/\nu$
U_j = mean jet exit velocity
U_∞ = mean freestream velocity
α = geometric angle of attack, deg
ν = kinematic viscosity
ρ = freestream fluid density

Subscripts

l.e. = leading-edge jet
t.e. = trailing-edge jet

Introduction

IN the present context, the term "circulation control" is used to denote a method of lift generation that utilizes tangential jet blowing over the upper surface of a rounded trailing-edge airfoil to set an effective Kutta condition by fixing the location of the boundary-layer separation points. This form of circulation control applied to rotorcraft offers the potential of relaxing the forward flight speed limitations due to conventional rotor retreating blade aerodynamic problems, i.e., lift loss due to reverse flow and dynamic stall. Realization of this potential is accomplished using rotor blade sections symmetric about midchord, with upper-surface leading- and trailing-edge jet blowing slots, permitting simultaneous blowing on each edge of the retreating blade, enabling the development of high lift coefficient values with the flow relative velocity coming from either direction (reverse or normal).

The circulation control concept of interest here initially was described in the literature by Cheeseman and Seed[1] in the 1960's. Since then, for the case of a two-dimensional airfoil under steady trailing-edge blowing, a substantial data base consisting of mean surface pressures and integrated forces and moments has been gathered for the purpose of performance evaluation. An extensive review of this work is provided by Wood and Nielsen.[2] Detailed flowfield studies are few and tend to pursue time-averaged measurements in the trailing-edge region (see, for example, Refs. 3 and 4). This attention to detail in the trailing-edge region has resulted in a neglect of the overall flowfield and its development, an aspect of concern to the present study.

Information concerning how the addition of leading-edge blowing affects the flowfield of a circulation control airfoil is extremely limited. The only published work that addresses the subject in some detail is that of Ottensoser,[5] whose data consisted of the usual mean surface pressure and wake rake measurements. His study was restricted in scope, however. This, along with the nature of his data, left certain aspects of the flow unresolved. Two of these aspects of concern to the present study regard the unsteady character of the flow and the behavior of the leading-edge jet.

This paper presents results of an experimental study undertaken in a water tunnel of the flowfield generated by a two-dimensional circulation control airfoil under steady leading- and trailing-edge blowing. The objective of this study was to fundamentally understand the overall flow structure generated and its relation to airfoil performance. Flow visualization as well as lift force measurements were used for this purpose.

Description of Experiment

The experiments were performed in the 8.4×12.0-in. (21×31-cm) rectangular closed-circuit water tunnel of the Army Aeroflightdynamics Directorate at the NASA Ames Research Center. A steel, two-dimensional, 4-in. (10.2-cm)-chord airfoil, horizontally spanning the test section, was tested (see Fig. 1). The airfoil had an uncambered elliptical section (20% thickness-to-chord ratio) with circular-arc leading and trailing edges; upper-surface leading- and trailing-edge jet slots; and dual plenum chambers. It must be noted that the airfoil section was chosen for its generic flow qualities rather than its high lift capability.

In the present study, the angle of attack was held constant at 0 deg and the jet slot height at $0.0015c$. Measurements were made of the mean and fluctuating forces at Reynolds numbers, based on chord, ranging from 1.2 to 3.9×10^5. Load cell transducers of the strain-gage-beam type were used to measure the lift force. The design of the model, force measurement apparatus, and jet flow control system used in the present test is described in detail by Panontin.[6] Flow visualization was performed over the same Reynolds number range as the force measurements and also for a Reynolds number of 3.4×10^4. Visualization of the jet flows was

Presented as Paper 87-0157 at the AIAA 25th Aerospace Sciences Meeting, Reno, NV, Jan. 12–15, 1987; received Oct. 20, 1987; revision received July 1, 1988.

*Research Scientist, Fluid Dynamics Research Branch.

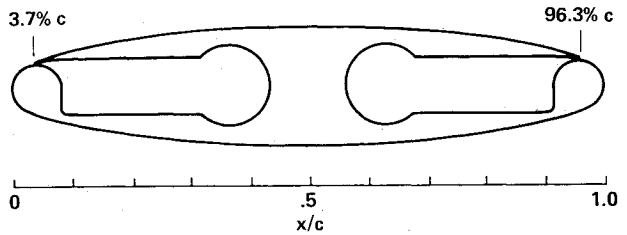

AIRFOIL PARAMETERS
CHORD – 4 in. (0.102 m)
THICKNESS – 0.2 c
JET SLOT HT. – 0.0015 c
L.E. & T.E. RADIUS – 0.04 c

Fig. 1 Airfoil geometry and parameters.

accomplished by introducing very small air bubbles[7] into the jet fluid prior to its discharge from the model. The outer flow was visualized using multiple filaments of hydrogen bubbles[8] generated by a kinked wire electrode vertically spanning the test section upstream of the model. Illumination was provided by a sheet of laser light vertically aligned parallel to the model's midspan and the flow. The observed flow patterns were recorded on a typical commercial-grade video system for later analysis.

A boundary-layer trip consisting of a spanwise strip of randomly distributed 0.027-in.-diam glass beads was located between the chordwise locations of 5 to 25% on both the upper and lower surfaces. The boundary layer was observed to be turbulent over the Reynolds number range of $1.2–3.9 \times 10^5$.

Note that all of the force curves displayed were obtained by running the load cell output directly to an analog plotter. No time averaging of the load cell output was done. Thus, the thickness of the lift-curve trace is an indication of the amplitude of the lift unsteadiness. Also noteworthy is that the force data presented were not corrected for blockage or jet momentum effects.

Experimental Results

The results are presented in two parts. The first describes the overall flow pattern and lift characteristics associated with trailing-edge blowing alone; the second describes the leading-edge flow patterns and lift characteristics associated with leading-edge blowing alone and simultaneously with trailing-edge blowing. Although, in detail, the interaction is somewhat complicated, the effect of leading-edge blowing can be looked on as a local modification of the flow pattern due to trailing-edge blowing.

Trailing-Edge Blowing Characteristics

An important feature of the flowfield in the present problem is entrainment by the jet. It is the mechanism that allows the jet to remain attached to the curved surface of the trailing edge even though large changes in direction may occur—a phenomenon known as the Coanda effect.[9] Therefore, it plays a primary role in determining the location where the jet separates from the surface.

Lift Characteristics

Typical lift characteristics associated with trailing-edge blowing alone are shown in Fig. 2. It is evident that as the jet blowing increases, the lift increases in a continuous fashion and the lift-curve slope decreases. A jet momentum value is reached, however, where the lift decreases abruptly. With further increase in jet momentum, the lift becomes highly unsteady and the mean lift level decreases.

Flow Visualization—Overall Flow Pattern

Based on the flow-visualization observations, the major features of the flow pattern associated with trailing-edge blowing are represented schematically in Fig. 3.

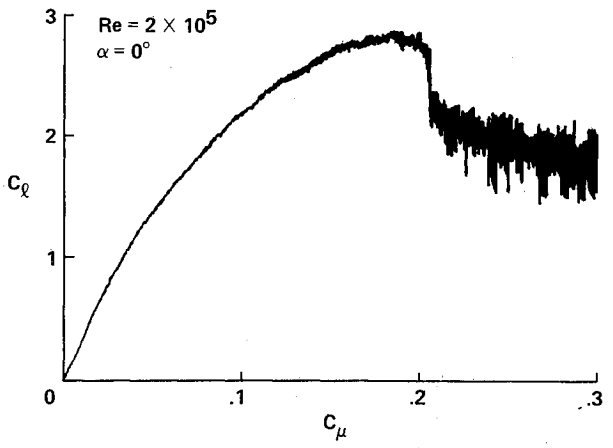

Fig. 2 Airfoil lift characteristics for trailing-edge blowing alone.

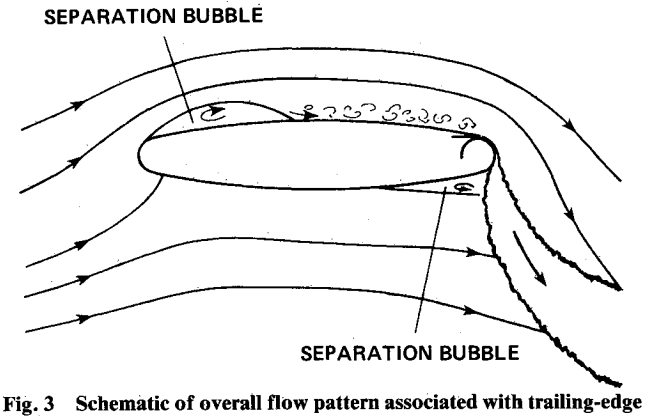

Fig. 3 Schematic of overall flow pattern associated with trailing-edge blowing.

Increasing jet momentum moves the jet separation point around the trailing edge toward the lower surface inducing circulation around the airfoil. This increased circulation is reflected in the flow pattern through an increase in the curvature of the streamlines. The pressure field attendant to the streamline curvature results in boundary-layer separation at the leading edge, with the resulting free shear layer reattaching to the airfoil surface at some distance from the leading edge, forming a separation bubble. As the trailing-edge blowing increases, the extent of this separation bubble increases, both in a direction normal to and along the airfoil surface. All during this growth, the wake of the separation bubble is unsteady, its scale visibly increasing as the jet momentum increases. At the same time, the jet itself, in the motion of its boundary and separation point location, displays more unsteadiness—"jitter"—than previously. This unsteadiness is also seen to increase as the jet momentum increases. It must be noted that visually there is a very strong impression that the bubble wake is affecting the jet entrainment process. The leading-edge separation bubble has received scant attention in the literature and the interaction of its wake with the trailing-edge jet flow has gone unnoticed.

Growth of the leading-edge separation bubble and its wake does not continue indefinitely; the bubble reaches its maximum size at a jet momentum coefficient of approximately 0.18, after first becoming visually noticeable at a jet momentum coefficient of approximately 0.14. Referring back to the lift curve (Fig. 2), it can be seen that the point at which the lift attains its maximum value correlates with the point at which the bubble reaches its maximum size and the bubble wake its maximum unsteadiness. Based on the above observations, it is interesting to speculate that the wake of the leading-edge separation bubble may be linked to the maximum lift value attainable in free air conditions, i.e., the occurrence of jet blowing stall.

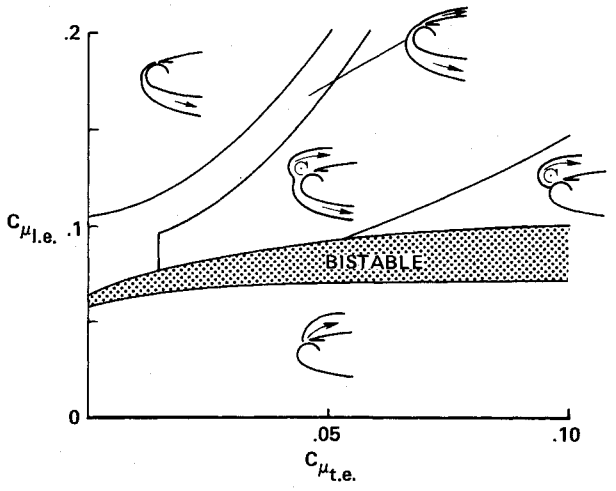

Fig. 4 Map of leading-edge jet behavior: $\alpha = 0$ deg.

Another consequence of the pressure field accompanying the increased streamline curvature is boundary-layer separation on the airfoil lower surface and the formation of a separation bubble ahead of the jet. The existence of this separation bubble appears to have been first noted by Kind[3] and more recently by Novak et al.[4] As the jet momentum is increased, a point is reached where entrainment of fluid by the jet reattaches the boundary layer and collapses the lower surface separation bubble. This process was seen to start at a jet momentum coefficient of approximately 0.13 and to be complete at a jet momentum coefficient of approximately 0.15.

Jet impingement on the lower test-section floor occurs for large values of jet blowing momentum. The result is a large blockage effect and the development of a highly unsteady flow condition in the test section that does not appear to have been noted previously in the literature. The occurrence of this condition correlates with the abrupt lift decrease and the corresponding high-lift unsteadiness displayed in Fig. 2. Thus, the abrupt lift loss displayed in the present results is probably due to wall interference and cannot be termed jet blowing stall.

One further point concerning wall interference needs to be made. The presence or absence of the tunnel walls does not alter the physics of the mechanism that causes the leading-edge separation bubble to occur initially—namely, the adverse pressure gradient imposed by the high streamline curvature at the leading edge.

Leading-Edge Blowing Characteristics

To a first approximation, the trailing-edge jet can be thought of as setting the flowfield that the leading-edge jet initially exits into. A feature that complicates this specific aspect of the overall flow is that the leading-edge jet exits against the outer flow. A competition therefore occurs between the momentum and pressure field of the outer flow and the momentum and entrainment of the leading-edge jet. The leading-edge flow structure is determined by the balance reached between these elements. Flow visualization in the present study indicates that entrainment by the leading-edge jet is a major determinant in setting the leading-edge flow structure.

One aspect of the flow connected with leading-edge blowing given particular attention in the present study concerns the behavior of the leading-edge jet. That the leading-edge jet exhibits different types of behavior was shown by Ottensoser[5] through indications in his surface pressure measurements. Unfortunately, these data proved insufficient to identify positively the types of behavior. Nevertheless, Ottensoser was led to hypothesize that two types of leading-edge jet behavior occur: one where the jet is able to overcome the outer flow and proceeds completely around the leading edge and over the lower surface, and the other where the outer flow overcomes the jet, folding it back completely over the upper surface. Visualization of the flow in the present study provided a direct means of identifying the leading-edge jet behavior and made it clear that the types of behavior are more than two.

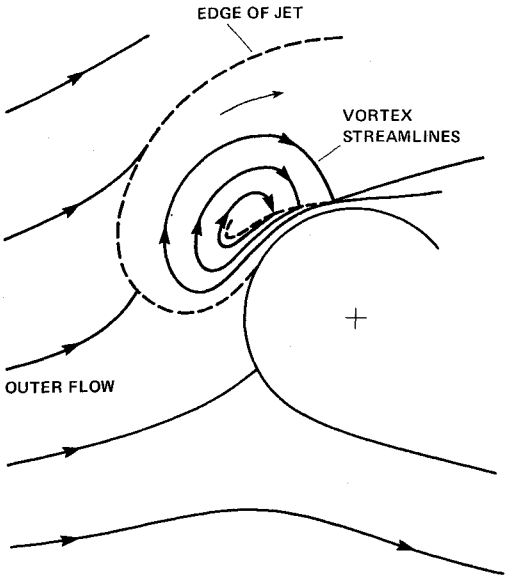

Fig. 5 Schematic of leading-edge flow pattern associated with "vortex" formation.

Flow Visualization—Leading-Edge Flow Pattern

The flow visualization revealed that, at low values of the leading-edge jet momentum coefficient, the leading-edge jet goes completely over the upper surface and, at high coefficient values, the leading-edge jet goes completely over the lower surface. For intermediate coefficient values, the leading-edge jet behavior is more complicated with the jet bifurcating, or becoming bistable. Here the term "bifurcation" is used to describe the division of the jet into two parts—one part proceeding over the upper surface, and the other proceeding over the lower surface. The term "bistable" is used to denote an unsteady condition. This point will be further elaborated on shortly.

A "map" of the leading-edge jet behavior was made through correlation of the flow-visualization observations with the leading- and trailing-edge jet momentum settings. This map is displayed in Fig. 4, where the observed types of leading-edge jet behavior are indicated schematically along with the boundaries that separate them. The first feature to note in the behavior map is the region connected with the bistable type of jet behavior that is seen to occur for an intermediate narrow range of $C_{\mu_{t.e.}}$ and to be nearly independent of $C_{\mu_{t.e.}}$. It is readily apparent that the bistable region extends as a band across the map, separating the only type of jet behavior that occurs for $C_{\mu_{l.e.}}$ less than the bistable range, the jet proceeding completely over the upper surface, from the more numerous and complex types of behavior that occur for $C_{\mu_{l.e.}}$ greater than the bistable range. The bistable type of behavior is an unsteady flow state where the structure of the leading-edge jet appears visually to move between the two steady flow states that border the bistable region along a line of constant $C_{\mu_{t.e.}}$. Four distinct types of jet behavior were observed for $C_{\mu_{l.e.}}$ greater than the bistable range. Two of them are of relatively simple nature, one with the jet proceeding completely over the lower surface, and the other with the jet bifurcating. The remaining two types of behavior observed occur at higher values of $C_{\mu_{t.e.}}$ than the previous two types and are composed of two of the behavior types already noted and an additional complicating feature, the formation of a circulatory flow pattern—namely, a "vortex." This visually prominent feature occurs for conditions where the majority of

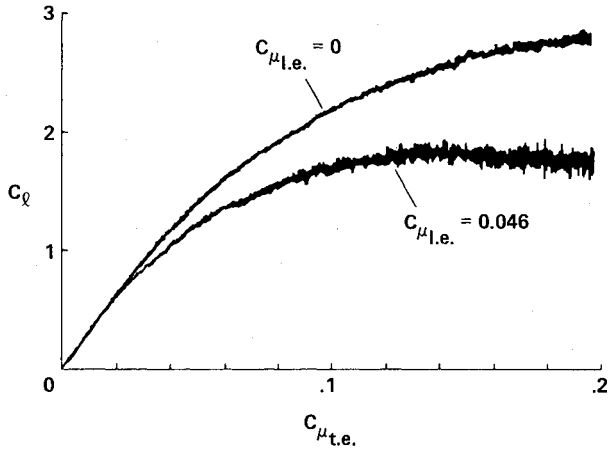

Fig. 6 Effect of trailing-edge blowing on lift characteristics: constant leading-edge blowing; $Re = 2.1 \times 10^5$, $\alpha = 0$ deg.

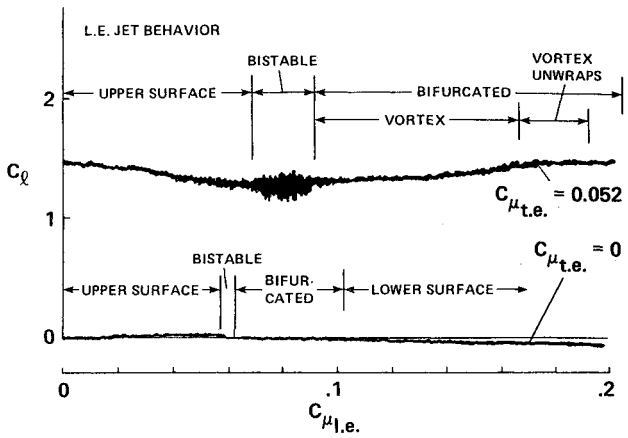

Fig. 7 Effect of leading-edge blowing on lift characteristics: constant trailing-edge blowing; $Re = 2.1 \times 10^5$, $\alpha = 0$ deg. Also indicated is the leading-edge jet behavior.

the jet folds back and proceeds over the upper surface after extending itself out over the airfoil nose. Entrainment by the jet of part of itself induces the circulatory flow pattern. A sketch illustrating this process is shown in Fig. 5. In addition, it was observed that starting in a region where the leading-edge vortex is formed and increasing the leading-edge jet momentum eventually results in reaching a state where the vortex is unable to maintain itself. During this transition to the new flow pattern, the vortex visually appears to unwrap in a highly unsteady process.

The map of leading-edge jet behavior is based on extensive data at a Reynolds number of 2.1×10^5. No Reynolds number dependence was found when comparison was made of that data to less extensive data taken throughout the Reynolds number range of 1.2 to 3.9×10^5. An interesting finding is that, with the boundary-layer trip removed, no change in the leading-edge behavior map was observed. The reason for this is that the leading-edge jet itself acts as a boundary-layer trip.

Lift Characteristics

The lift characteristics for simultaneous leading- and trailing-edge blowing were obtained by holding the momentum of one jet constant and varying the momentum of the other jet. A typical result of this procedure is shown in Fig. 6, where the lift coefficient is plotted as a function of the trailing-edge jet momentum coefficient for two constant values of the leading-edge jet momentum coefficient, 0 and 0.046. For both leading-edge values, the lift increases with increasing trailing-edge blowing. However, it is clear that the presence of leading-edge blowing results in a lift decrease in comparison to the trailing-edge blowing-alone case. This finding is in agreement with that of Ottensoser.[5] Also of note is the increased unsteadiness of the lift in the leading-edge blowing case.

A representative example of reversing the preceding procedure is shown in Fig. 7, where the effect of leading-edge jet momentum on the lift is displayed for constant trailing-edge jet momentum coefficients of 0 and 0.052. Also indicated in Fig. 7 is the leading-edge jet behavior. In the presence of trailing-edge blowing, the lift is approximately constant for small to moderate jet momentum coefficients and is lower than the lift generated for jet momentum coefficient values outside that range. The width of the reduced lift zone increases as the trailing-edge jet momentum increases. A feature to particularly note in the reduced lift zone is a pronounced unsteadiness in the lift that occurs over a small jet momentum coefficient range that corresponds to the bistable region displayed in Fig. 4. Another particularly noteworthy feature is the lift behavior in the vortex unwrap zone. The leading-edge flow pattern was seen to be highly unsteady as the vortex unwraps, yet this unsteadiness was not reflected to the same degree in the lift measurements. In the absence of trailing-edge blowing, low lift is generated. Yet, the low lift generated does exhibit behavior of note: an abrupt decrease, though slight, in the lift and a change in the sign of the lift-curve slope when the jet becomes bistable.

Concluding Remarks

The flow-visualization results of the present study have revealed that the leading-edge jet behavior is far more complicated than hypothesized by previous investigators. It was found that, at low values of leading-edge jet momentum, the leading-edge jet falls back and proceeds completely over the upper surface; at high momentum values, the jet proceeds completely over the lower surface; and, at intermediate momentum values, the jet bifurcates, proceeding over the upper and lower surfaces simultaneously. A prominent feature of the leading-edge flowfield for certain values of leading- and trailing-edge jet momentum is a circulatory flow pattern—a vortex—induced by jet entrainment. In addition, it was found that simultaneous steady blowing can result in an unsteady flow condition for certain values of leading- and trailing-edge jet momentum. Two unsteady flow conditions were observed. One, defined as being bistable, where the leading-edge jet moves back and forth between two steady flow states, and another being when the leading-edge vortex is no longer able to maintain itself and unwraps. It will be interesting to see if present computational methods will be able to capture these complex flow patterns.

The lift was found to slightly decrease under simultaneous blowing in comparison to trailing-edge blowing alone. This finding is in agreement with previous investigators and further validates the proposed use of simultaneous blowing in rotorcraft applications. Of the two unsteady flow conditions found, only one, the bistable condition, is reflected as increased unsteadiness in the lift. It remains to be seen whether the existence of this region of unsteady lift will have a negative impact on the use of simultaneous blowing.

For trailing-edge blowing alone, a new feature was identified: an interaction between the wake of the leading-edge separation bubble and the trailing-edge jet flow that results in increased unsteadiness of the flow and consequently in the lift. The maximum intensity of this interaction was also found to correlate with the maximum lift attained.

A question that naturally arises is how the preceding observations, particularly those concerning leading-edge jet behavior, depend on airfoil geometry. Since the present experiment was restricted to one geometry, this remains an open question.

Acknowledgments

The author wishes to thank the Army Aeroflightdynamics Directorate for the use of its water tunnel and the assistance of its staff in its operation, particularly R. Losee. Appreciation is also extended to T. Panontin and J. Brown for engineering design; A. Ayoub for beneficial discussions; S. K. Robinson for his helpful comments after reviewing the first draft of this paper; J. B. Scott for fabrication of the model; and N. Wood and L. Rodman for advice helpful in the model's design.

References

[1]Cheeseman, I. C. and Seed, A. R., "The Application of Circulation Control by Blowing to Helicopter Rotors," *Journal of the Royal Aeronautical Society,* Vol. 71, No. 679, July 1967, pp. 451–467.

[2]Wood, N. J. and Nielsen, J. N., "Circulation Control Airfoils—Past, Present, Future," AIAA Paper 85-0204, Jan. 1985.

[3]Kind, R. J., "A Proposed Method of Circulation Control," Ph.D. Dissertation, Univ. of Cambridge, England, June 1967.

[4]Novak, C. J., Cornelius, K. C., and Roads, R. K., "Experimental Investigations of the Circular Wall Jet on a Circulation Control Airfoil," AIAA Paper 87-0155, Jan. 1987.

[5]Ottensoser, J., "Two-Dimensional Subsonic Evaluation of a 15-Percent Thick Circulation Control Airfoil with Slots at Both Leading and Trailing Edges," David Taylor Naval Ship R&D Center, Rept. 4456, July 1974.

[6]Panontin, T. L., "Circulation Control Lift Generation Experiment: Hardware Development," 19th Aerospace Mechanisms Symposium, NASA Ames Research Center, Moffett Field, CA, May 1985.

[7]Neuwerth, G., "Stroemungssichtbarmachung in Wasserkanaelen mittels eines Verfahrens zur Erzeugung kleinster Luftblaeschen," *Zeitschrift fuer Flugwissenschaften und Weltraumforschung,* Vol. 9, May–June 1985, pp. 187–189.

[8]Clutter, D. W. and Smith, A. M. O., "Flow Visualization by Electrolysis of Water," *Aerospace Engineering,* Vol. 20, Jan. 1961.

[9]Wille, R. and Fernholz, H., "Report on the First European Mechanics Colloquium on the Coanda Effect," *Journal of Fluid Mechanics,* Vol. 23, Pt. 4, 1965, pp. 801–819.